J Chin Med Assoc

ORIGINAL ARTICLE

Macular ganglion cell-inner plexiform vs retinal nerve fiber layer measurement to detect early glaucoma with superior or inferior hemifield defects

Mei-Ju Chen[a,b], Yu-Fan Chang[a,c], Yih-Shiuan Kuo[a], Chih-Chien Hsu[a,c], Yu-Chieh Ko[a,b,c], Catherine Jui-Ling Liu[a,b,*]

[a]Department of Ophthalmology, Taipei Veterans General Hospital, Taipei, Taiwan, ROC; [b]School of Medicine, National Yang-Ming University, Taipei, Taiwan, ROC; [c]Institute of Clinical Medicine, National Yang-Ming University, Taipei, Taiwan, ROC

Abstract

Background: To compare the diagnostic ability of Cirrus high-definition spectral-domain optical coherence tomography measurements of the macular ganglion cell-inner plexiform layer (GCIPL) vs the circumferential retinal nerve fiber layer (cpRNFL) to detect early glaucoma with hemifield visual field (VF) defects.

Methods: This prospective study included 96 patients with primary open-angle glaucoma (48 with superior hemifield defects and 48 with inferior hemifield defects) and 48 normal control subjects. All glaucomatous eyes had a mean deviation of the VF defect ≥–6.0 dB confined to one hemifield. cpRNFL and GCIPL thicknesses were recorded. Area under the receiver operating characteristic curve (AUROC) was calculated for each parameter and compared.

Results: All GCIPL parameters and most cpRNFL parameters (except at the nasal quadrant, and 2-, 3-, and 4-o'clock sectors) were significantly lower in glaucomatous eyes vs those in normal controls. In the superior hemifield defect group, the best discriminating parameters were 7-o'clock-sector cpRNFL thickness (AUROC value, 0.963), inferior cpRNFL thickness (0.926), and inferotemporal GCIPL thickness (0.923). Performance was comparable between the best measures of GCIPL analysis (inferotemporal GCIPL thickness) and those of cpRNFL (7-o'clock-sector thickness, $p = 0.28$). In the inferior hemifield defect group, the best discriminating parameters were 11- and 10-o'clock-sector cpRNFL thickness (0.940 and 0.904, respectively), and average cpRNFL thickness (0.909). Performance was comparable between the best measures from each method (superotemporal GCIPL thickness vs. 11-o'clock-sector cpRNFL thickness [0.857 vs 0.940, $p = 0.07$]).

Conclusion: Diagnostic abilities of GCIPL parameters and cpRNFL parameters for early glaucoma were comparable for eyes with either superior or inferior hemifield VF defects.

Keywords: Glaucoma; Open-angle glaucoma; Optical coherence tomography

1. INTRODUCTION

Glaucoma is characterized by the progressive death of retinal ganglion cells (RGCs) and loss of their axons, with corresponding visual field (VF) defects. Spectral-domain optical coherence tomography (OCT) has revealed thinning of the inner retina or RGC complex within the macular area in early glaucoma[1,2] and preperimetric glaucoma.[3] Studies using Cirrus high-definition (HD)-OCT (Carl Zeiss Meditec, Dublin, CA, USA) measurements of the macular ganglion cell-inner plexiform layer (GCIPL) and the circumferential peripapillary retinal nerve fiber layer (cpRNFL) for early glaucoma detection report that GCIPL results are equal or inferior to cpRNFL outcomes.[4–9] However, little is known about the diagnostic ability of Cirrus HD-OCT measurements of GCIPL vs cpRNFL in cases of early glaucoma with localized hemifield VF defects.

GCIPL measurements are acquired via macular scanning of a fovea-centered elliptical annulus; thus, the likelihood of detecting abnormal GCIPL thickness is influenced by the anatomic location of RGC loss relative to the fovea. Because the fovea is usually located below the retina's horizontal meridian, asymmetric distribution of the retinal nerve fiber layer (RNFL) bundles often occurs between the superior and inferior retina. Therefore, the diagnostic ability of the GCIPL parameters might be different according to the location of hemifield defects. To our knowledge, only few studies have reported this issue. In the present study, we aimed to determine whether diagnostic abilities differed between GCIPL vs cpRNFL among early glaucomatous eyes with localized superior or inferior hemifield VF defects.

2. METHODS

2.1. Subjects

We recruited patients with primary open-angle glaucoma (POAG) who visited the outpatient clinic of Taipei Veterans General Hospital between June 2013 and December 2014. All POAG patients were treated and regularly followed up during

*Address correspondence: Dr. Catherine Ju-Ling Liu, Department of Ophthalmology, Taipei Veterans General Hospital. 201, Section 2, Shi-Pai Road, Taipei 112, Taiwan, ROC. E-mail address: jlliu@vghtpe.gov.tw (C. J.-L. Liu)

Conflicts of interest: The authors declare that they have no conflicts of interest related to the subject matter or materials discussed in this article.

Journal of Chinese Medical Association. (2019) 82: 335-339.

Received September 19, 2017; accepted August 22, 2018.

doi: 10.1097/JCMA.0000000000000037.

the study period. We also enrolled healthy control subjects by recruiting normal volunteers in our hospital. Healthy subjects included hospital staff and patients who visited our clinic for annual health examination. The study protocol was approved by the institutional review board of our hospital and was designed in accordance with the Declaration of Helsinki. Written informed consent was obtained from all subjects.

POAG was diagnosed on the basis of characteristic glaucomatous changes of the optic nerve head (ONH) and/or RNFL, and reliable glaucomatous VF defects in eyes with open anterior chamber angle. Neuroretinal rim thinning, notching, and/or excavation were considered as characteristic glaucomatous ONH changes. To meet the diagnostic criteria, RNFL defects had to conform with the distribution pattern and correspond to the ONH changes. Glaucomatous VF was defined as three contiguous nonedge points within the same hemifield showing a pattern standard deviation (PSD) p value of <0.05 and with at least one point having a p value of <0.01 by two reliable VF tests or classified as outside normal limits by a glaucoma hemifield test.[10] A reliable VF test was defined as having a fixation loss rate <25%, false positive rate <15%, and false negative rate <15%.

VF defects were subdivided into two categories according to the location of VF damage. A central scotoma was defined as a scotoma within the central 12 degrees of fixation, with at least one point having a p value of <0.01 within the central six degrees of fixation on the PSD plot. A localized peripheral scotoma was defined as a scotoma outside of the central six degrees of fixation and with no VF abnormality within the central six degrees of fixation on the PSD plot.[11]

All subjects underwent a comprehensive ophthalmic examination, including assessment of best-corrected visual acuity, automated refraction and keratometry, Goldman applanation tonometry (GAT), slit-lamp examination, gonioscopy, dilated fundus examination, colored and red-free fundus photography, and automated VF examination (Humphrey 24-2 SITA standard algorithm). Axial length (AL) was measured with IOLMaster (Carl Zeiss Meditec), and central corneal thickness (CCT) was determined using a DGH 55 Pachmate (DGH Technology, Exton, PA, USA). To be enrolled in the study, subjects had to meet the following criteria: age ≥20 years, best-corrected visual acuity ≥20/40, open-angle structure upon gonioscopic examination, and astigmatism ≤3 diopters (D). POAG patients were required to have an intraocular pressure (IOP) <24 mmHg as assessed by GAT and a diagnosis of early glaucoma based on a VF mean deviation (MD) >−6 dB.[12] Considering the effect of CCT on IOP measurement, the value of 24 mmHg was chosen to ensure well-controlled IOPs in POAG patients. Normal subjects were required to have an IOP <22 mmHg as assessed by GAT and no abnormal ocular findings, including no glaucomatous changes in the ONH and VF. Eyes were excluded if they showed retinal or neurologic diseases, ocular inflammation, prior ocular surgery within 3 months, prior refractive surgery, or concurrent disease that could interfere with IOP measurement, OCT imaging, or cause VF defects.

2.2. Optical coherence topography measurement

Cirrus HD-OCT (Carl Zeiss Meditec) was performed following pupillary dilation. The Cirrus HD-OCT Optic Disc Cube 200 × 200 protocol was used to measure average cpRNFL thickness and cpRNFL thickness in quadrants and in 12 clock-hour sectors. The Macular Cube 200 × 200 protocol was used to calculate average, minimum, and regional GCIPL thickness in six wedge-shaped sectors. Images were excluded if they exhibited signal strength <7, motion artifact, poor centration, segmentation error, artifacts caused by ocular pathology, or missing data on the peripapillary region. There was a time interval of <3 months between HD-OCT and other ophthalmic examinations (eg, VF).

2.3. Statistical methods

For the glaucoma group, the eye with a better MD of VF was included in the statistical analyses. For normal subjects, if both eyes were eligible, one eye was randomly chosen. Statistical analyses were performed using the statistical package for the social science (SPSS) statistical package (SPSS, Inc., Chicago, IL, USA). For continuous variables, the normality of data distribution was verified using the Shapiro-Wilk test. To analyze differences between the glaucoma and normal groups, we used the Student's t test for normally distributed data and the Mann-Whitney U test for nonnormally distributed data. The chi-square test was used to compare the sex ratio and the central scotoma-to-peripheral scotoma ratio. To evaluate the ability of each parameter to discriminate early glaucoma from normal eyes, we calculated the area under the receiver operating characteristic curve (AUROC) and made comparisons using the method of DeLong et al.[13] A p value of <0.05 was considered as statistically significant.

3. RESULTS

This study included 96 POAG eyes (48 superior hemifield defects and 48 inferior hemifield defects) and 48 normal control eyes. Table 1 shows the demographic and clinical characteristics of the subjects. There were no significant intergroup differences in age, sex, spherical equivalence, AL, IOP, or CCT. The glaucoma

Table 1

Demographic and clinical characteristics of the study population

	Normal (n = 48)	Superior hemifield defect (n = 48)	Inferior hemifield defect (n = 48)	p^a	p^b	p^c
Age, y	50.6 ± 12.5	54.3 ± 12.6	53.6 ± 15.4	0.158	0.308	0.806
Male/Female	22/26	27/21	20/28	0.307	0.681	0.153
SE, D	−3.76 ± 4.13	−4.10 ± 4.10	−3.78 ± 3.94	0.610	0.829	0.724
AL, mm	25.07 ± 1.55	25.50 ± 1.83	25.50 ± 1.68	0.237	0.136	0.975
IOP, mmHg	16.2 ± 3.4	17.3 ± 3.3	17.0 ± 3.3	0.105	0.248	0.620
CCT, μm	551 ± 20	566 ± 36	562 ± 37	0.069	0.205	0.859
Vertical C/D	0.57 ± 0.17	0.79 ± 0.10	0.77 ± 0.12	<0.001	<0.001	0.421
MD, dB	−1.20 ± 1.55	−3.02 ± 1.43	−3.20 ±1.02	<0.001	<0.001	0.394
PSD, dB	1.89 ± 0.94	4.23 ± 1.87	3.67 ± 1.97	<0.001	<0.001	0.084
VFI, %	96.3 ± 14.3	93.3 ± 4.2	94.7 ± 3.1	<0.001	<0.001	0.113
Central scotoma /peripheral scotoma[d]		20/28	11/37			0.025

[a]Comparison between superior hemifield defect glaucoma and normal control eyes.

[b]Comparison between inferior hemifield defect glaucoma and normal control eyes.

[c]Comparison between superior hemifield defect glaucoma and inferior hemifield defect glaucoma.

[d]The ratio of central vs peripheral locations of VF defects in superior or inferior hemifield glaucoma.

AL = axial length; CCT = central corneal thickness; C/D = cup-to-disc ratio; D = diopter; IOP = intraocular pressure; MD = mean deviation; PSD = pattern standard deviation; SE = spherical equivalent; VFI = visual field index.

Table 2

Comparison of GCIPL and cpRNFL thickness measurements between three groups

	Normal (n = 48)	Superior hemifield defect (n = 48)	Inferior hemifield defect (n = 48)	p^a	p^b	p^c
cpRNFL thickness, μm						
Average	96.1 ± 9.0	81.9 ± 11.3	77.1 ± 1.7	<0.001	<0.001	0.042
Superior	115.7 ± 18.3	106.7 ± 18.8	82.3 ± 17.6	0.020	<0.001	<0.001
Nasal	65.1 ± 10.3	65.9 ± 11.0	62.3 ± 10.1	0.711	0.171	0.091
Inferior	120.9 ± 16.4	82.9 ± 18.9	100.0 ± 18.5	<0.001	<0.001	<0.001
Temporal	81.4 ± 12.4	71.8 ± 13..2	63.2 ± 13.1	<0.001	<0.001	0.002
cpRNFL clock hours thickness, μm						
12 superior	108.5 ± 26.1	103.6 ± 26.5	76.5 ± 21.2	0.273	<0.001	<0.001
1	98.7 ± 23.6	89.8 ± 23.1	85.7 ± 20.5	0.075	0.005	0.568
2	73.2 ± 13.2	72.6 ± 11.9	69.5 ± 14.9	0.778	0.202	0.281
3 nasal	60.3 ± 11.3	59.7 ± 12.5	59.7 ± 11.4	0.824	0.808	0.860
4	62.7 ± 12.2	65.7 ± 14.7	57.6 ± 10.3	0.276	0.027	0.007
5	88.8 ± 16.3	85.3 ± 19.7	77.0 ± 15.9	0.357	0.001	0.025
6 inferior	125.7 ± 24.7	84.6 ± 26.3	101.3 ± 23.1	<0.001	<0.001	<0.001
7	148.5 ± 20.8	78.8 ± 27.9	121.8 ± 26.9	<0.001	<0.001	<0.001
8	85.0 ± 16.4	64.2 ± 17.2	67.6 ± 15.6	<0.001	<0.001	0.242
9 temporal	63.8 ± 11.0	61.7 ± 11.7	54.0 ± 10.1	0.356	<0.001	0.001
10	89.3 ± 21.9	68.1 ± 19.6	85.0 ± 23.2	0.045	<0.001	<0.001
11	139.5 ± 21.5	126.8 ± 25.4	83.7 ± 26.1	0.009	<0.001	<0.001
GCIPL thickness, μm						
Average	80.7 ± 6.4	71.5 ± 8.3	72.3 ± 7.6	<0.001	<0.001	0.628
Minimum	77.4 ± 10.1	60.2 ± 12.4	65.1 ± 10.2	<0.001	<0.001	0.038
Superonasal	82.9 ± 7.2	79.0 ± 12.2	75.4 ± 10.9	0.100	<0.001	0.140
Superior	80.9 ± 6.6	76.8 ± 10.0	71.5 ± 9.5	0.036	<0.001	0.010
Superotemporal	80.0 ± 5.5	75.6 ± 7.9	69.4 ± 8.0	0.002	<0.001	<0.001
Inferotemporal	80.9 ± 5.8	62.4 ± 10.2	72.1 ± 8.8	<0.001	<0.001	<0.001
Inferior	77.8 ± 8.5	63.8 ± 10.6	70.8 ± 8.8	<0.001	<0.001	0.001
Inferonasal	81.2 ± 7.5	73.2 ± 11.3	74.6 ± 9.8	<0.001	<0.001	0.728

[a]Comparison between superior hemifield defect glaucoma and normal control eyes.

[b]Comparison between inferior hemifield defect glaucoma and normal control eyes.

[c]Comparison between superior hemifield defect glaucoma and inferior hemifield defect glaucoma.

CpRNFL = circumferential peripapillary retinal nerve fiber layer; GCIPL = ganglion cell-inner plexiform layer.

groups and normal controls significantly differed in vertical cup-to-disc ratio, MD, PSD, and VFI. The inferior hemifield defect group had predominantly peripheral scotoma, while the superior hemifield defect group had a comparable number of central and peripheral scotomas. The central scotoma-to-peripheral scotoma ratio was significantly lower in the inferior hemifield VF defect group compared to that in the superior hemifield defect group ($p = 0.025$).

All GCIPL and most cpRNFL (except at the nasal quadrant and the 2- to 4-o'clock sectors) thicknesses measured by HD-OCT were significantly lower in POAG eyes compared to normal eyes (Table 2). Significant differences in cpRNFL were noted between the superior and inferior hemifield glaucoma groups for the measurements in the superior, inferior, and temporal quadrants and at most of the clock hours, except for clock sectors 1 to 3 and 8. The superotemporal, inferotemporal, and inferior GCIPL measurements also significantly differed between the superior and inferior hemifield glaucoma groups. Additionally, the perimetrically normal hemifields of glaucomatous eyes showed significantly decreased GCIPL and cpRNFL thicknesses compared to the corresponding hemifields of normal controls, particularly in the inferior hemifield glaucoma group.

In the superior hemifield defect glaucoma group, the 7-o'clock-sector RNFL thickness had the largest AUROC value (0.963), followed by inferior RNFL thickness (0.926), inferotemporal GCIPL thickness (0.923), and minimum GCIPL thickness (0.877) (Fig. 1). Performances were comparable between the best measures from each method (inferotemporal GCIPL thickness vs 7-o'clock-sector RNFL thickness; $p = 0.28$). In the inferior hemifield defect glaucoma group, the best parameters for discriminating normal eyes from glaucomatous eyes were the 11-o'clock-sector RNFL thickness (0.940), average RNFL thickness (0.909), 10-o'clock-sector RNFL thickness (0.904), and superior RNFL thickness (0.898; Fig. 2). Performances were also comparable between the best-performing GCIPL outcome (superotemporal GCIPL thickness, 0.857) and the best measure of the RNFL analysis (11-o'clock-sector RNFL thickness, 0.940; $p = 0.07$). Also, the best diagnostic parameter of the GCIPL analysis in the superior hemifield glaucoma group (inferotemporal GCIPL thickness, 0.923) was comparable to that of the inferior hemifield glaucoma group (superotemporal GCIPL thickness, 0.857; $p = 0.167$). The best measure in the RNFL analysis of the superior hemifield glaucoma group (7-o'clock-sector RNFL thickness, 0.963) showed a similar diagnostic ability to that of the inferior hemifield glaucoma group (11-o'clock-sector RNFL thickness, 0.940; $p = 0.489$).

4. DISCUSSION

Our findings demonstrated that GCIPL parameters performed as well as cpRNFL parameters for early glaucoma diagnosis among eyes with either localized superior hemifield or inferior hemifield defect. We also observed significantly decreased GCIPL and cpRNFL thicknesses in areas corresponding to the perimetrically uninvolved hemifields of glaucomatous eyes compared to their counterparts in normal control eyes. This finding is in line with previous reports[14, 15] and supports prior evidence that glaucomatous structural changes often precede functional changes, as demonstrated by standard automated perimetry.[16, 17]

In contrast to our present findings, Kim et al.[18] performed a retrospective study of glaucomatous eyes with superior or inferior visual hemifield defects and reported that GCIPL parameters showed inferior diagnostic performance compared to cpRNFL parameters in eyes with inferior hemifield defects.

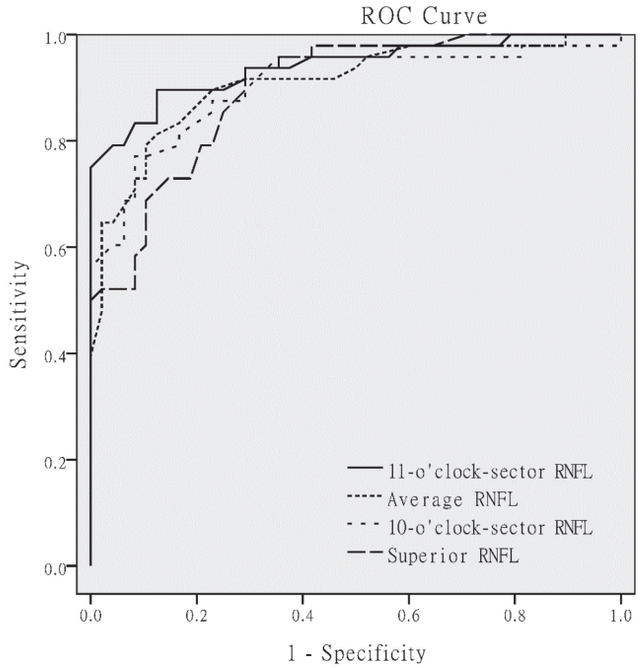

Fig. 1 Area under the receiver operating characteristic curve (AUROC) values for the superior hemifield defect glaucoma group. The 7-o'clock-sector retinal nerve fiber layer (RNFL) thickness showed the largest AUROC value (0.963), followed by inferior RNFL thickness (0.926), inferotemporal ganglion cell-inner plexiform layer (GCIPL) thickness (0.923), and minimum GCIPL thickness (0.877).

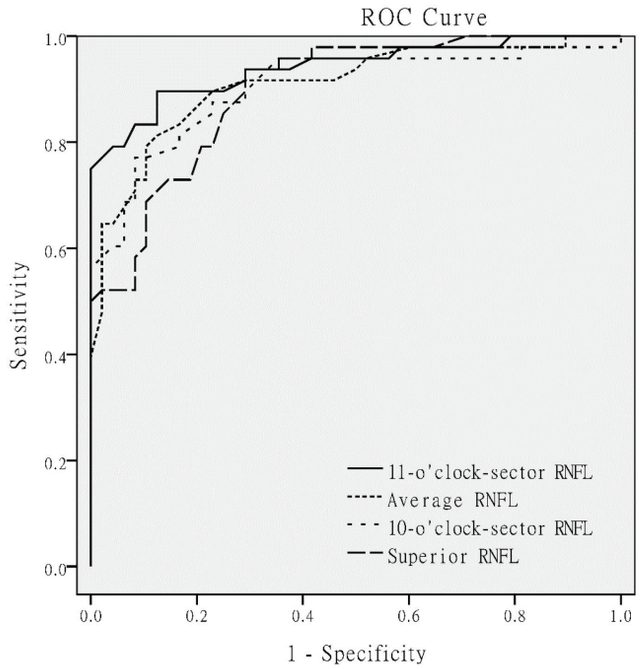

Fig. 2 Area under the receiver operating characteristic curve (AUROC) values for the inferior hemifield defect glaucoma group. The best parameters for discriminating normal eyes from glaucomatous eyes were the 11-o'clock-sector retinal nerve fiber layer (RNFL) thickness (0.940), average RNFL thickness (0.909), 10-o'clock-sector RNFL thickness (0.904), and superior RNFL thickness (0.898).

Notably, the diagnostic performance of the GCIPL algorithm may be impacted by the location of either a central or a peripheral VF defect,[19] in addition to the hemifield distribution. GCIPL parameters perform better than cpRNFL parameters in eyes with paracentral VF defects, while cpRNFL parameters outperform GCIPL parameters in eyes with peripheral VF defects. Kim et al.[18] did not report the distribution of central vs peripheral locations of VF defects in their study. However, in our study, the inferior hemifield defect group had predominantly peripheral scotomas; thus, it is unlikely that a difference in VF location was the reason for disparity between results of these two studies.

Several studies show that the superotemporal and inferotemporal RNFL bundles tend to temporally converge with increasing myopia.[20–22] Our present study enrolled glaucoma patients and normal control subjects with a mean refractive error of −3.9 ± 4.1 D. This is substantially different from the mean refractive error of −0.4 ± 1.4 D previously reported by Kim et al.[18] A smaller angular distance between the fovea and RNFL defect could increase the likelihood of RGC loss being detected by GCIPL parameters in the elliptical macular scanning area of 14.13 mm^2. Another possible explanation for the differing results between studies is that we analyzed the outcomes of OCT and VF examinations performed within 3 months of each other, while Kim et al.[18] did not report the time interval between OCT imaging acquisition and VF test conduction.

Interestingly, in our study, the superior hemifield defect group included a comparable number of eyes with central and peripheral scotomas, while the inferior hemifield defect group had markedly fewer eyes with central scotomas than peripheral scotomas. Previous reports have also described unequal presentation of central scotomas between the superior and inferior hemifields.[23,24] Hood et al.[25] performed a study focusing on glaucomatous damage of the macula and demonstrated the projection of RGCs from a small (cecocentral) region of the inferior macula and all of the superior macula to the temporal quadrant—a region that is less susceptible to glaucomatous damage. This may explain why the central VF is more commonly involved in glaucomatous eyes with localized superior hemifield defects than with inferior hemifield defects.

Our present study had several limitations. First, the sample size was relatively small, precluding further subgroup analysis of eyes with central and peripheral scotoma between the two different hemifield defect groups. Second, all the study subjects were of Taiwanese ethnicity and the results cannot be extrapolated to patients of other ethnicities. Third, the diagnostic performance of HD-OCT could be affected by age, refractive error, AL, and VFI. However, we recruited early glaucoma patients and age- and refractive error-matched normal control subjects to minimize the confounding effect of these factors. Lastly, we defined early glaucoma based on VF findings, which inherently excluded eyes with preperimetric glaucoma. Not study has yet identified the earliest changes detectable by HD-OCT in eyes with preperimetric damage limited to the superior or inferior ONH. Despite these limitations, our present results are relevant to clinical practice with regard to discriminating between early glaucoma and normal eyes.

In conclusion, GCIPL parameters and cpRNFL parameters showed comparable diagnostic abilities among patients with early glaucoma with either superior or inferior hemifield VF defects. The measurement of macular GCIPL may further enhance the use of OCT for early glaucoma detection.

REFERENCES

1. Tan O, Chopra V, Lu AT, Schuman JS, Ishikawa H, Wollstein G, et al. Detection of macular ganglion cell loss in glaucoma by Fourier-domain optical coherence tomography. *Ophthalmology* 2009;**116**:2305–14.
2. Kotera Y, Hangai M, Hirose F, Mori S, Yoshimura N. Three-dimensional imaging of macular inner structures in glaucoma by using spectral-domain optical coherence tomography. *Invest Ophthalmol Vis Sci* 2011;**52**:1412–21.
3. Lisboa R, Paranhos A, Jr., Weinreb RN, Zangwill LM, Leite MT, Medeiros FA. Comparison of different spectral domain OCT scanning protocols for diagnosing preperimetric glaucoma. *Invest Ophthalmol Vis Sci* 2013;**54**:3417–25.

4. Mwanza JC, Durbin MK, Budenz DL, Sayyad FE, Chang RT, Neelakantan A, et al. Glaucoma diagnostic accuracy of ganglion cell-inner plexiform layer thickness: comparison with nerve fiber layer and optic nerve head. *Ophthalmology* 2012;**119**:1151–8.
5. Kotowski J, Folio LS, Wollstein G, Ishikawa H, Ling Y, Bilonick RA, et al. Glaucoma discrimination of segmented cirrus spectral domain optical coherence tomography (SD-OCT) macular scans. *Br J Ophthalmol* 2012;**96**:1420–5.
6. Nouri-Mahdavi K, Nowroozizadeh S, Nassiri N, Cirineo N, Knipping S, Giaconi J, et al. Macular ganglion cell/inner plexiform layer measurements by spectral domain optical coherence tomography for detection of early glaucoma and comparison to retinal nerve fiber layer measurements. *Am J Ophthalmol* 2013;**156**:1297–307.
7. Jeoung JW, Choi YJ, Park KH, Kim DM. Macular ganglion cell imaging study: glaucoma diagnostic accuracy of spectral-domain optical coherence tomography. *Invest Ophthalmol Vis Sci* 2013;**54**:4422–9.
8. Begum VU, Addepalli UK, Yadav RK, Shankar K, Senthil S, Garudadri CS et al. Ganglion cell-inner plexiform layer thickness of high definition optical coherence tomography in perimetric and preperimetric glaucoma. *Invest Ophthalmol Vis Sci* 2014;**55**:4768–75.
9. Kim MJ, Park KH, Yoo BW, Jeoung JW, Kim HC, Kim DM. Comparison of macular GCIPL and peripapillary RNFL deviation maps for detection of glaucomatous eye with localized RNFL defect. *Acta Ophthalmol* 2015;**93**:e22–8.
10. Budenz DL *Altas of visual fields*. Philadelphia, PA: Lippincott-Raven; 1997.
11. Cho HK, Lee J, Lee M, Kee C. Initial central scotomas vs peripheral scotomas in normal-tension glaucoma: clinical characteristics and progression rates. *Eye* 2014;**28**:303–11.
12. Hodapp E, Parrish RK, Anderson DA *Clinical decisions in glaucoma*. St. Louis, MO: Mosby-Year Book; 1993.
13. DeLong ER, DeLong DM, Clarke-Pearson DL. Comparing the areas under two or more correlated receiver operating characteristic curves: a nonparametric approach. *Biometrics* 1988;**44**:837–45.
14. Na JH, Kook MS, Lee Y, Yu SJ, Choi J. Detection of macular and circumpapillary structural loss in normal hemifield areas of glaucomatous eyes with localized visual field defects using spectral-domain optical coherence tomography. *Graefes Arch clin Exp Ophthalmol* 2012;**250**: 595–602.
15. Takagi ST, Kita Y, Yagi F, Tomita G. Macular retinal ganglion cell complex damage in the apparently normal visual field of glaucomatous eyes with hemifield defects. *J Glaucoma* 2012;**21**:318–25.
16. Sommer A, Katz J, Quigley HA, Miller NR, Robin AL, Richter RC, et al. Clinically detectable nerve fiber atrophy precedes the onset of glaucomatous field loss. *Arch Ophthalmol* 1991;**109**:77–83.
17. Tuulonen A, Airaksinen PJ. Initial glaucomatous optic disk and retinal nerve fiber layer abnormalities and their progression. *Am J Ophthalmol* 1991;**111**:485–90.
18. Kim HS, Yang H, Lee TH, Lee KH. Diagnostic value of ganglion cell-inner plexiform layer thickness in glaucoma with superior or inferior visual hemifield defects. *J Glaucoma* 2016;**25**:472–6.
19. Shin HY, Park HL, Jung KI, Choi JA, Park CK. Glaucoma diagnostic ability of ganglion cell-inner plexiform layer thickness differs according to the location of visual field loss. *Ophthalmology* 2014;**121**: 93–9.
20. Kim MJ, Lee EJ, Kim TW. Peripapillary retinal nerve fibre layer thickness profile in subjects with myopia measured using the Stratus optical coherence tomography. *Br J Ophthalmol* 2010;**94**:115–20.
21. Kang SH, Hong SW, Im SK, Lee SH, Ahn MD. Effect of myopia on the thickness of the retinal nerve fiber layer measured by Cirrus HD optical coherence tomography. *Invest Ophthalmol Vis Sci* 2010;**51**:4075–83.
22. Leung CK, Yu M, Weinreb RN, Mak HK, Lai G, Ye Cet al. Retinal nerve fiber layer imaging with spectral-domain optical coherence tomography: interpreting the RNFL maps in healthy myopic eyes. *Invest Ophthalmol Vis Sci* 2012;**53**:7194–200.
23. Park SC, De Moraes CG, Teng CC, Tello C, Liebmann JM, Ritch R. Initial parafoveal versus peripheral scotomas in glaucoma: risk factors and visual field characteristics. *Ophthalmology* 2011;**118**:1782–9.
24. Jung KI, Park HY, Park CK. Characteristics of optic disc morphology in glaucoma patients with parafoveal scotoma compared to peripheral scotoma. *Invest Ophthalmol Vis Sci* 2012;**53**:4813–20.
25. Hood DC, Raza AS, de Moraes CG, Liebmann JM, Ritch R.Glaucomatous damage of the macula. *Prog Retin Eye Res* 2013;**32**:1–21.